Instituto Universitario de Bio-Orgánica Antonio González
Universidad de La Laguna

Máster en Biomedicina

BioLab

EARLY PHARMACOLOGICAL PROFILING OF BIOACTIVE NATURAL PRODUCTS AND THEIR ANALOGUES

Perfil farmacológico temprano de productos naturales bioactivos y sus análogos sintéticos

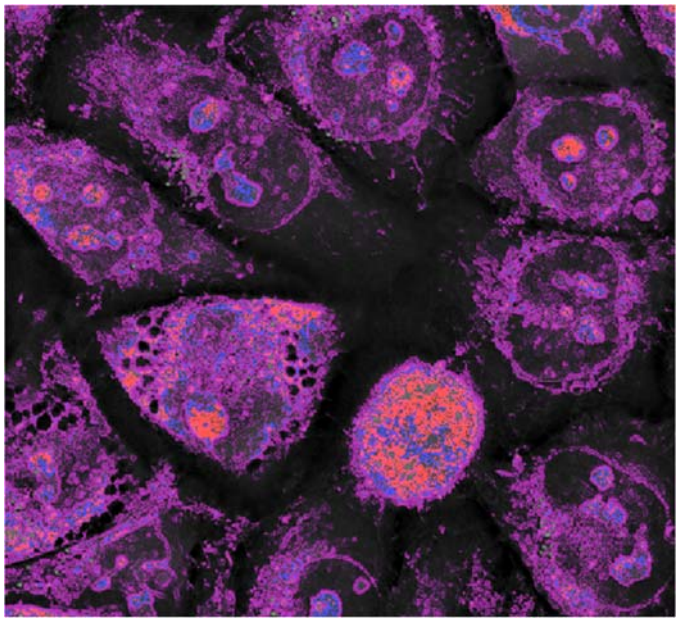

Trabajo de Fin de Máster

Aday González Bakker

Tutorizado por Dr. José M. Padrón y Dr. Guido Santos Rosales

Máster en Biomedicina

Junio 2022

La presente memoria de investigación ha sido realizada por Aday González Bakker durante el curso académico 2021-2022 en las instalaciones del Instituto Universitario de Bio-Orgánica "Antonio González" (IUBO-AG) y bajo la dirección del Dr. José M. Padrón y del Dr. Guido Santos Rosales. El trabajo forma parte de la línea de investigación *Diseño, descubrimiento y evaluación de fármacos anticancerígenos* y ha sido financiado en parte por el proyecto METABOLITOS BIOACTIVOS PROCEDENTES DE ECOSISTEMAS DE VERACRUZ (MÉXICO) concedido mediante resolución 78/2021 del Vicerrectorado de Proyección, Internacionalización y Cooperación.

La Laguna, a 8 de junio de 2022.

TABLE OF CONTENTS

ABSTRACT

Bioprospection has a very important role in the discovery of compounds with antitumor activity. A large number of the actual anticancer drugs has a natural origin. Due to the high biodiversity around the world, which leads to new chemical structures (with new targets) and the general multi-faceted mechanisms, makes necessary the use of phenotypic profiling to discover and define the target of these compounds. Phenotypic drug discovery requires the use of different assays to narrow down the possible mechanism of action such as the evaluation of cell migration and phenotypic changes in the cell. In this study, we carried out an optimization of in vitro wound healing assay and tested a panel of natural extracts of *Hypericum* genus to evaluate cell migration. We determined that in lung cancer cells A549, a serum concentration of 1% is suitable to evaluate cell migration. We observed differential effect of the extracts on migration with a considerable inhibition in cell migration by the hydroalcoholic extract of *H. grandifolium*. In addition, we designed a preliminary model based on Fourier's Transform to use Nanolive's CX-A imaging and analysis system for target prediction. The designed model was able to preliminary cluster microtubule affecting drugs with similar mechanism of action to those of vinblastine and colchicine.

RESUMEN

La bioprospección juega un papel muy importante en el descubrimiento de compuestos con actividad antitumoral. Muchos de los compuestos quimioterápicos actuales están relacionados con productos naturales. Debido a la alta biodiversidad alrededor del mundo que supone la aparición de nuevas estructuras químicas (con nuevas dianas) y a la general actividad multifacética de los compuestos naturales, es necesario el estudio del perfil fenotípico de fármacos para descubrir estos compuestos y definir su diana. El descubrimiento fenotípico de fármacos requiere del uso de diferentes ensayos para acotar el posible mecanismo de acción, por ejemplo, la evaluación de la migración celular o cambios fenotípicos en la célula. En este trabajo realizamos la optimización del ensayo de herida in vitro y evaluamos el efecto de diferentes extractos vegetales del género *Hypericum.* Determinamos que la línea celular A549 con 1% de suero es el modelo óptimo para evaluar la migración. Observamos efectos diferenciales de los extractos sobre la migración con una inhibición considerable por el extracto hidroalcohólico de *H. grandifolium*. Además, diseñamos un modelo preliminar basado en la transformada de Fourier para usar el sistema de imagen y análisis CX-A de Nanolive para predecir dianas. El modelo bioinformático diseñado fue capaz de agrupar compuestos con mecanismo de acción similar contra los microtúbulos (vinblastina y colchicina).

INTRODUCTION

Bioprospecting is the systematic search, classification and investigation of new sources of chemical compounds, genes, proteins, microorganisms and other products with high added value, based on the biological diversity of a region. This holistic search within the ecosystem allows the economic, scientific, technological and human development of geographic regions of high diversity. In addition, these products from Nature with an inherent high added value, contribute significantly to protect and restore biodiversity through social awareness and regulations. Current bioprospecting methodologies are classified according to the objective of the search. Thus, we distinguish three closely related branches: a) chemical, b) ecological, and c) genetic bioprospecting [1]. Among them, chemical bioprospecting, based on the study of the different living kingdoms, has led to the discovery of drugs with therapeutic, nutraceutical, cosmetic, and agrochemical applications [2].

The plant kingdom has great importance in research supported by the fact that many plants are used in popular medicine for their medicinal properties and also offer a great diversity of specialized metabolites, which makes them a practically inexhaustible source of molecules with the most diverse applications [3]. Noteworthy, plants represent one of the sources of greatest diversity, with more than 300,000 species, and only 20% of terrestrial plants have been evaluated for potential uses. Consequently, plant species represent a source of raw materials for the discovery of high added value compounds. The historical successes in drug discovery based on natural products would suggest that there should be a continued appetite for accessing natural products for use in drug discovery programs. A key issue unresolved in bioprospecting is benefit-sharing. Drugs directly or indirectly derived from bioresources are anticipated to contribute significantly to the conservation of biodiversity in source countries, and to the development of indigenous knowledge holder communities. In our group, we aim to generate a bank of extracts from the pharmacognostic study of native and non-native plant species of the Canary Islands, with the aim of expanding knowledge about the drug-botanical potential of the plants that develop in the Canary Islands. The biobank will regionally address a global problem that is the need to contribute to the conservation and sustainable use of biodiversity, natural resources and ecosystem services in the Canary Islands and, therefore, in the Macaronesian region.

Bioprospection and cancer treatment

Natural products have marked the history of anticancer drug discovery. A number of widely-used anticancer therapeutics originate from natural sources, such as irinotecan, vincristine, etoposide and paclitaxel from plants, actinomycin D and mitomycin C from bacteria as well as marine-derived bleomycin [4]. Some of these compounds are still the mainstay of cancer therapy and will continue to play an important role in cancer treatment.

The emergence of molecularly targeted therapies has reshaped the landscape of cancer treatment. As the way the field develops, the interest of natural products research has been drawn to into molecularly targeted drug hunting. In this way, many natural products have been found to be active against specific targets. For example, eucalyptin A, which is derived from the fruits of *Eucalyptus globulus* Labill, was found to exhibit potent inhibitory effect on HGF/c-Met axis [5].

Nowadays, the prevailing precision medicines in cancer therapy underscores the necessity to fully understand the molecular basis of anticancer drugs [4]. This has supposed a change from phenotypic screen to target-based screen (TBS). The phenotypic screen is a discovery process that identifies chemical entities that have desirable biological (phenotypic) effects on cells or organisms without having prior knowledge of their biochemical activity or mode of action against a specific molecular target [6]. In contrast, TBS is believed to be more efficient and cost-effective to identify drugs with the clarified mechanism of action [7]. However, TBS may not be the best system to manifest the advantage of natural products in cancer treatment [4]. This is related to complexity of this disease. TBS assays will show specific interaction with a concrete target. In cancer, a complex interplay of various internal and environmental factors at different levels occurs [8]. The inhibition of one single target will hardly have the desired therapeutically effect or it could result in resistance phenomenon more easily. The advantage of natural products could be related to multiple targeting of the compound and the possible presence of new chemical entities with new structures with potential antitumor activity. In this way, integrating both types of screening seem the most efficient to find new and effective antitumoral compounds. The integration of both methods requires the generation of efficient selection systems. Direct target determination by assays like the use of inmovilized compounds to study protein interactions based on affinity [9], or enzimatic assays to see inhibition of certain enzimes, are complicated to use to determine the target of a bioactive compound. Because of the high diversity of targets and the higher cost of these kind of assays require to use more easy assays that help to reduce possible targets.

Evaluating diferent characteristics like cell mobility, phenotypic response, or the expresion of certain proteins will help us to generate phenotypic profiles that will reduce the number of posible targets before making direct target assay. This aproach can make target definition of a compound most cost-effective.

Cell migration

Cell migration is the ability of a cancer cell to undergo movement and invasion allowing it to relocate within the tissues [10]. For example, these processes allow neoplastic cells to enter lymphatic and blood vessels for dissemination into the circulation, and then undergo metastatic growth in distant organs. The epithelial-to-mesenchymal transition (EMT) is responsible for the disruption of cell–cell adhesion and cellular polarity, remodeling of the cytoskeleton, and changes in cell–matrix adhesion [11]. Because of this it is associated with improvement in migratory and invasive properties.

Evaluating cell migration in vitro can give us information about possible targets of new antitumor compounds. For example, it has been described that compounds affecting microtubules inhibit cell migration in in vitro wound healing assay [12]. In this study, we propose the optimization of in vitro wound healing assay to study cell migration and evaluate the effect on cell migration of different bioactive natural extracts.

Live cell imaging and machine learning in phenotypic drug discovery

The role of artificial intelligence (AI) in pharmaceutical research and drug discovery is getting increasing attention [13]. Machine learning algorithms in structure recognition, classification, conformation simulation, library design, and activity prediction are a potent tool to assess the discovery and characterization of new (natural and synthetic) anticancer compounds. For instance, the Developmental Therapeutics Program (DTP) from de National Cancer Institute (NCI) has developed an algorithm named COMPARE, which based on their 60 cell lines screening panel is able to predict possible targets [14]. Using the parameters of the antiproliferative activity (GI_{50}, TGI, or LC_{50}) for each cell line a fingerprint is generated. Then, the system ranks the already tested compounds based in the similarity to this fingerprint. Compounds with similar fingerprint may possess the same mechanism of action [15], whilst new fingerprints or patterns should appear if tested compounds display an unprecedented mechanism of action.

The evaluation of compounds in such a big panel is not affordable for a regular research group. However, the lack of cell lines can be compensated using data from other assays. Attending to this, Nanolive's platform CX-A is an automated 3D label-free live cell imaging system with a highly integrated multi-parametric image analysis system. The device offers a potential alternative since it generates measurements for each cell of the sample under evaluation. This gives us the chance to evaluate phenotypic responses to a compound not only at endpoint but during all de study. This These results combined with the correct algorithm will potentially be able to predict action mechanism of new compounds. In this study, we propose an algorithm to use this imaging system as tool for the study of the mechanism that can led to the prediction of the biological target.

HYPOTHESIS

Products from Nature, and particularly from the biodiversity, represent a sustainable source of potential high added value compounds with pharmacological uses. Natural products are strongly ligated to cancer treatment, being bioactive by themselves or as a base to obtain derivatives with antitumor activity. Due to the high biodiversity around the world, new and different chemical compounds can be obtained from these organisms. Our hypothesis is that bioprospection is a strongly useful source of new chemical entities with antitumor activity. The target definition of these compounds under study can be assessed by phenotypic changes using live cell imaging.

OBJECTIVES

The main purpose of this work is to identify new mechanisms of action for antitumor compounds using phenotypic profiling. To achieve this goal, we define the following objectives.

1. To optimize different techniques to narrow down possible targets.
2. To perform phenotypic profiling of different natural bioactive compounds.
3. To design an algorithm for target prediction using life cell imaging.

MATERIALS AND METHODS

1. Cell lines and culture

1.1. Cell lines

We selected a panel of human solid tumour cell lines comprising lung (A549, and SW1573), and cervix (HeLa) cancer cell lines. The cell lines were kindly provided by Prof. G. J. Peters (VUMC, Amsterdam), Prof. A. Pandiella (CIC, Salamanca), Dr. R. Freire (HUC, Tenerife) and CEAMED S.A. (Tenerife).

1.2. Cell passage and maintenance

Cells were grown in RPMI 1640 medium supplemented with 2 mM glutamine, 5% fetal bovine serum (FBS), and 100 U/mL penicillin and 0.1 mg/mL streptomycin as antibiotics. They were incubated at 37ºC, in humidified atmosphere 5% CO_2 and maintained at low passage.

2. Cell migration assay

2.1. Optimization of the wound healing assay

To study cell migration, we carried out optimization of the wound healing assay, an easy method to evaluate cell mobility in vitro **¡Error! No se encuentra el origen de la referencia.**. First, we trypsinised cell cultures from A549, SW1573 and HeLa to prepare single cell suspensions. After cell counting, we prepared the appropriate dilution for seeding at a density of 30,000 cells/well. We seeded 1 mL onto a 24 well plate and incubate the cells until they reached 80-90% confluence. Afterwards, a mark was drawn on the outside bottom of each well. This will enable to find the same point (reference point) when taking pictures. For each well, a scratch on the cell culture was made perpendicularly to the mark using a sterile p200 tip. Then medium was replaced for fresh medium with different FBS concentrations (0, 1, 2.5 and 5%) with or without Ara-c (final concentration of 1 µM). Pictures were taken with a brightfield microscope (Axiovert 40 CFL, Zeiss, Germany) at one magnification (5X) using the software ZEN 2012 (blue edition v1.1.0.0) at different time intervals (0, 6, and 24 hours from the scratch).

For the quantification of cell migration, the free software Tscratch developed by CSElab **¡Error! No se encuentra el origen de la referencia.** was used. We stablished the

threshold to separate manually for each image the low-intensity open area and the high-intensity covered area. The algorithm provided the results expressed as scratch area percentage.

2.2. Statistical analysis of the wound healing assay

Statistical analysis was carried out using analysis software Jamovi version 1.6.23. [18]. The wound area at the corresponding time intervals were compared using paired samples T-test. After calculating relative wound closure, ANOVA analysis was performed to evaluate the effect of the different treatments on cell mobility. To confirm normality of the data and homogeneity of variances, Shapiro-Wilk and Levene's tests were used respectively. Tukey's post-Hoc test was used in pair-to-pair comparation.

2.3. Cell migration inhibition

To evaluate cell mobility inhibition by test extracts, A549 cells were used. The in vitro wound healing assay was performed as described before using 2.5% FBS with or without selected extracts. Extracts were assayed at 2 concentrations, 100 µg/mL and 50 µg/mL. Images were taken and quantified as described before.

2.4. Quantification of cell growth

To quantify cell growth effect during the optimization process of in vitro wound healing, we used crystal violet (CV) staining in 24 well plates recreating in vitro wound healing conditions and staining the cells at selected time intervals. Cells were incubated with absolute methanol for 3 minutes. Then, they were stained using a 0.5% CV solution for 5 minutes. After that, CV was re-dissolved with a 1% SDS in PBS solution until it was completely solubilized. Then, the absorbance at 590 nm was measured in a microplate reader (BioTek PowerWave XS).

3. Live cell imaging

3.1. Image acquisition

To evaluate drug induced phenotypic changes related to different biochemical mechanisms of action, live cell microscopy was performed using CX-A label free cell imaging system from Nanolive SA. First, SW1573 cells were trypsinised and after counting 100,000 cells were seeded on 35 mm high glass bottom µ-dish from IBIDI. After 24 h, medium was changed for RPMI 1640 without phenol red, and cells were treated with

different drugs targeting microtubules (paclitaxel, vinblastine, and colchicine) at a concentration of 1 µM. Each treatment was repeated once but measures were obtained for each cell in imaging area. Right after that, the plates were placed in the CX-A and images from a 236µm x 236µm area were taken every 3 minutes for 20 h.

4. Bioinformatic analysis and prediction algorithm design

After image acquisition, Eve segmentation and analysis software from Nanolive SA was used to evaluate 11 phenotypic related parameters including Cell area [μm^2], Cell area [%], Cell perimeter, Cell eccentricity, Cell granularity, Cell compacteness, Cell form factor, Cell extent, Mean refraction index, Average dry mass density [pg / µm3] and Dry mass [pg]. The measurements were obtained for each cell at all imaging cycles (the initial cell amount of the field area was in the range 15–25 cells) for each treatment.

For the design of the model, we used Rstudio version 2022.02.2+485 [19]. Data directly obtained from Nanolive's Eve analysis software was recasted using function `recast` from package `reshape2` to obtain time series of the variables for each cell. After calculating the mean at each time interval, the dataset was centred using function `scale`. Then Fourier transform (FT) was calculated using function `fft`, which is a mathematical transform that decomposes functions depending on time into functions depending on temporal frequency [20] (Figure 1). After this transformation, period and phase values for every variable were obtained. For the cluster analysis, the frequency and phase corresponding with the maximal amplitude of the FT of the time series, for each variable, where used.

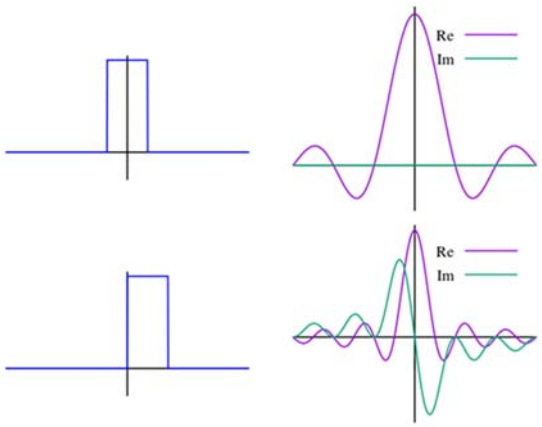

Figure 1. Schematic representation explaining Fourier´s transform application. The top row shows a unit pulse as a function of time (f(t)) and its Fourier transform as a function of frequency ($\hat{f}(\omega)$). The bottom row shows a delayed unit pulse as a function of time (g(t)) and its Fourier transform as a function of frequency ($\hat{g}(\omega)$).

RESULTS AND DISCUSSION

Compounds isolated from natural sources are likely to have antitumor activity. The high number of molecules that can be obtained from this source makes phenotypic drug discovery the best approach to find and characterize the activity of these drugs. This requires optimization of methods and techniques to define targets and mechanisms of action.

1. In vitro wound healing optimization

Cell mobility is an interesting feature to evaluate because of the implication of cell migration in early stages of metastasis or valuable information to narrow down possible targets. In vitro wound healing is an easy and cheap way to preliminarily assess cellular movement. However, this technique has been described using different conditions depending on the author [21] [22]. In this work, we studied the effect of diverse variables trying to optimize this technique.

The cell lines selected for this assay were A549, SW1573 and HeLa. A549 is a non-small cell lung cancer (NSCLC), the most common type of lung cancer and one of the most aggressive type of cancers worldwide [23] because of invasiveness of near tissues and metastasis. A549 has all the features of EMT transformed cells. This makes A549 an commonly used model to evaluate cell migration [24]. SW1573 is also a NSCLC cell line [25]. This common origin with A549, makes SW1573 an interesting cell type to evaluate with this technique. Finally, HeLa is epithelioid cervix carcinoma and it was selected because of the fast growth of this cell line. This will make it fast to reach the high confluence necessary for the wound healing assay.

The most limiting barriers using this technique are the effect of cell growth, which can make overestimate wound closure. Since we want to visualize migration and not growth as the reason of wound closure, it became necessary to reduce cell growth after the scratch without inducing nutrient depletion that could affect normal cell functions such as migration [21]. To reduce this effect, different serum concentrations were evaluated to find the one that accomplishes this condition. We also evaluated the use of Ara-c, a G_1-arresting drug that binds to cyclin-dependent kinase 4 (CDK4), an inhibitor of the formation of the cell cycle-dependent CDK4/cyclin D1 complex, subsequently leading to cell cycle arrest in the G_1/S phase [26]. This could potentially avoid cell growth while keeping cells in good conditions to close the wound.

Another limiting factor into consideration is the effect of cell death induced by the tested drug. A high death rate could result in reduction of wound closure without being related to inhibition of cell mobility. To avoid this effect, drugs should be tested at a low concentration. Another way to reduce high cell death effect can be reducing the time of exposure. Thus, measuring the wound closure at 6 h instead of higher intervals, i.e. 12 or 24 h, where death will be presumably higher. To find if migration could be measured at lower time intervals paired samples T-test were performed comparing areas at 0 and 6 h for the three cell lines. As shown in Table 1, in the three cell models and at all serum concentrations, the areas are significantly different. This result indicates that measuring the wound after 6 h of inducing the scratch will allow to determine wound closure.

Table 1. Paired samples T-test from wound area at different FBS concentrations.

Cell line	FBS (%)	Area t=0	Area t=6	statistic	df	p *
HeLa	0	23.8 ± 6.8	20.3 ± 7.0	4.76	8.00	0.001
	1	24.6 ± 6.0	16.3 ± 5.9	6.13	8.00	< 0.001
	2.5	24.2 ± 3.7	16.3 ± 4.4	4.53	7.00	0.003
	5	22.8 ± 5.3	15.4 ± 5.0	3.74	8.00	0.006
A549	0	18.2 ± 3.0	16.6 ± 3.0	7.80	8.00	< 0.001
	1	17.1 ± 3.3	13.9 ± 2.9	11.91	8.00	< 0.001
	2.5	18.0 ± 3.5	15.3 ± 2.8	7.02	8.00	< 0.001
	5	17.5 ± 3.3	15.4 ± 3.2	5.98	8.00	< 0.001
SW1573	0	18.2 ± 3.0	16.6 ± 3.0	5.05	8.00	< 0.001
	1	17.1 ± 3.0	13.9 ± 2.9	4.90	8.00	0.001
	2.5	18.0 ± 4.0	15.3 ± 2.8	5.10	8.00	< 0.001
	5	17.5 ± 3.0	15.4 ± 3.2	3.34	8.00	0.010

Measurements were compared independently to avoid Family-Wise Error Rate. Differences were considered significative (*) when $p < 0.05$.

The possibility to run the assay 6 h after wound induction obtaining significantly different areas, make possible to run experiments in less time. This reduces cell death and growth effects when studying the wound closure. Thus, we calculated migration at 6 h as a measure of *relative closure percentage* (Equation 1). ANOVA analysis was used to observe if there was a significative effect of FBS concentration in migration for each cell line.

$$Wound\ Closure\% = \left(\frac{A_{t=0} - A_{t=\Delta t}}{A_{t=0}}\right) x100\% \qquad \textbf{Equation 1}$$

1.1. Migration of HeLa cells

After confirming normality of the data and homogeneity of the variances, the ANOVA showed that there was a significant effect of FBS concentration on closure. Attending to Tukey's post hoc test, we observed that the closure was significantly less in the medium without FBS, as expected, but no significant differences were found between the rest of serum amounts (Table 2). This was unexpected because it would mean that cell growth effect is the same at all serum concentrations and we could only differentiate cell migration in the absence of FBS. However, CV staining (Figure 2) showed that there is an important cell growth effect at all serum concentrations but 0%. Based on our previous experience working with this cell line, we know that it has a very strong and fast growth which has been reflected in this assay. Even at lower serum concentrations, we could see considerable cell growth. The only way to evaluate cell migration with this method using HeLa cells is removing completely serum from the medium otherwise closure will be highly influenced by cell increment.

Table 2. Descriptive statistics for wound closure assays in HeLa cells 6 h after the wound.

Serum concentration (%)	N	Mean	SD	SE
0.0[b]	9	16.3	8.81	2.94
1.0[a]	9	34.9	9.31	3.10
2.5[a]	9	33.3	14.41	4.80
5.0[a]	9	35.1	9.52	3.17

(a) $p > 0.05$, (b) $p < 0.05$.

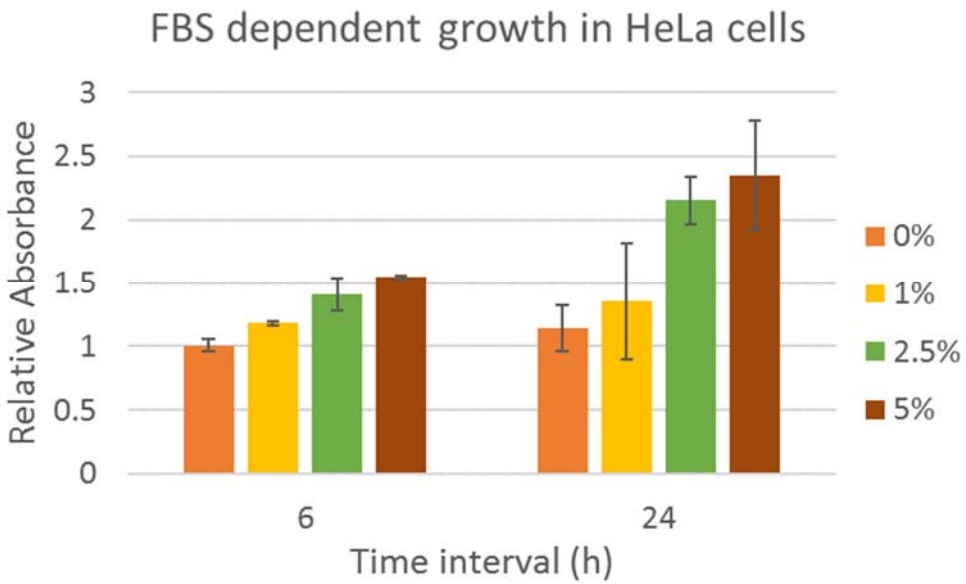

Figure 2. Growth effect of FBS in HeLa cells.

1.2. Migration of A549 cells

Attending to the ANOVA analysis of the effect of serum in wound healing for A549, we could observe that depletion of serum reduces significatively ($p<0.05$) wound closure. Significant differences were found between 0% FBS and the remaining conditions. We also found significant differences in 5% FBS treatment with respect to 1% and 2.5% FBS ($p<0.001$ and $p=0.043$, respectively) but no difference was found between 1 and 2.5% ($p=0.213$) (Table 3). In this case, we could see that there are significant differences in the closure comparing cells in growing conditions (5% FBS) and lower serum concentrations. However, the closure is still significatively higher than at 0% FBS. This suggests that the 1% or 2.5% are probably the serum concentrations where we are observing the highest closure with the less cell-growth effect. This was confirmed with the CV staining (Figure 3) where we observed that at 6 h there was almost not increment in absorbance in comparison with the wells stained at 0 h, while at 5% FBS the increment was 30% with respect to initial absorbance. This would confirm that there is no cell growth at 6 h for A549 with 1–2.5% FBS, while there is a better closure than removing completely the FBS.

Table 3. Descriptive statistics for wound closure assays in A549 cells 6 h after the wound.

Serum concentration (%)	N	Mean	SD	SE
0.0[b]	8	3.74	2.77	0.978
1.0[a]	9	13.35	3.93	1.309
2.5[a]	9	18.22	5.49	1.831
5.0c	9	25.03	7.20	2.402

(a) $p>0.05$, (b, c) $p<0.05$.

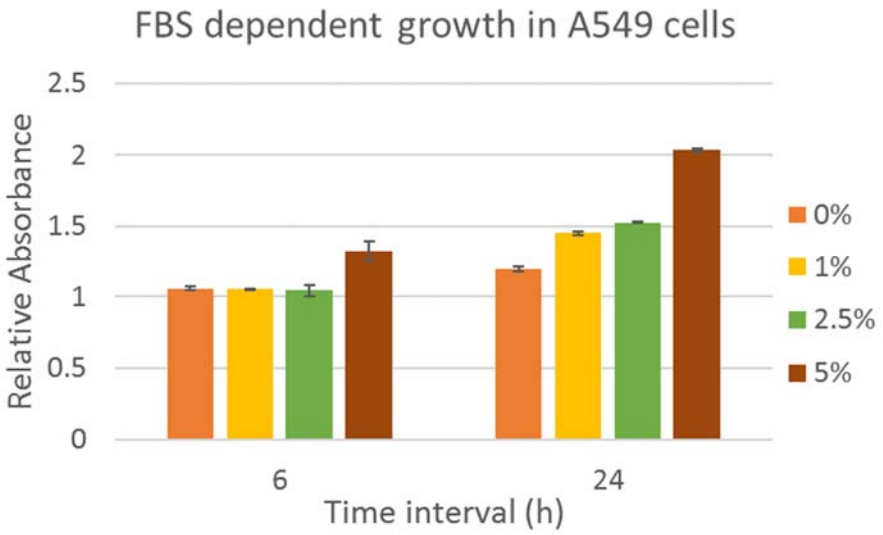

Figure 3. Growth effect of FBS on A549 cells.

1.3. Migration of SW1573 cells

The ANOVA analysis showed that there is a significant effect of serum concentration on wound closure ($p<0.05$). When considering the post hoc test, we observed that at 0% of FBS significant less closure than the rest of the concentrations occurs, but no significant differences were found between 1 and 2.5 or 5% treatments ($p=1.000$ and $p=0.930$, respectively). Neither between 2.5 nor 5% FBS ($p=0.940$) (Table 4). Attending to the descriptive of the data, it seems that wound closure in SW1573 is not influenced by the increment of FBS since there were no significant differences. The slightly higher closure with 5% FBS is probably due to an increment in cell number which we confirmed with CV staining, where we could observe a slight increment over the rest of the conditions tested (Figure 4).

Table 4. Descriptive statistics for wound closure assays in SW1573 cells 6 h after the wound.

Serum concentration (%)	N	Mean	SD	SE
0.0[b]	10	8.35	4.98	1.58
1.0[a]	9	17.84	7.28	2.43
2.5[a]	9	17.91	7.90	2.63
5.0[a]	9	19.85	9.08	3.03

(a) $p>0.05$, (b) $p<0.05$.

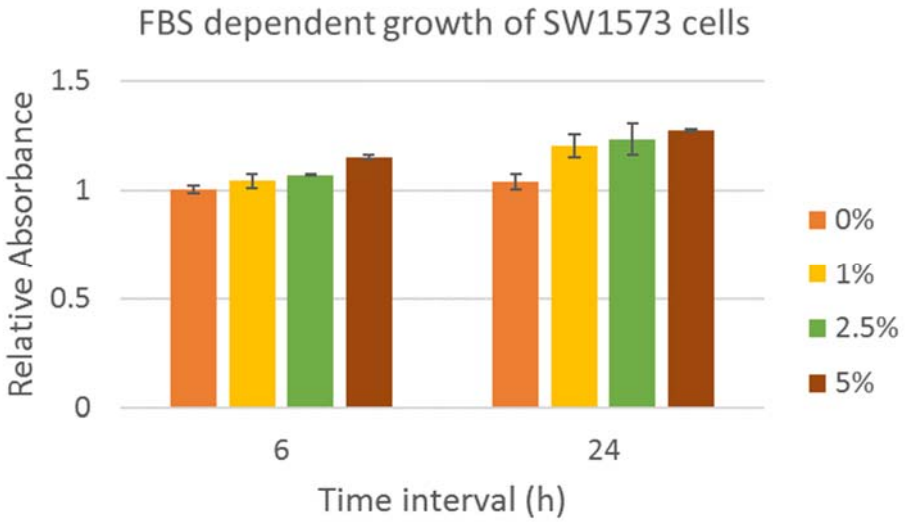

Figure 4. Growth effect of FBS on SW1573 cells.

In summary, high variability was exhibited by SW1573 cells in relation to A549 or HeLa, suggesting that it might not be an appropriate model to evaluate cell migration with this technique. Comparing HeLa with A549, we observed that cell migration in HeLa cells

must be evaluated removing the serum to avoid cell growth influence. With A549 cells we found using 1% or 2.5% as the serum amount were the closure is the highest while cell growth is kept to a minimum. Even though closure in both cell lines under these conditions can be similar, the deviation in HeLa at 0% FBS is almost 50% of the mean. This high variability can reduce the sensitivity to detect cell migration inhibition. Importantly, in A549 cells with 1 and 2.5% FBS the deviation is not that large. Therefore, the use of A549 cells either at 1 or 2.5% FBS seems the best conditions to run this assay. The election of 1% FBS would also save more serum.

1.4. Use of Ara-C

Ara-C is a commonly used selective inhibitor of DNA synthesis, which does not inhibit RNA synthesis. Ara-C prevents cell proliferation in migration assays. We tested the effect on wound closure at a fix dose of 1µM, on different cell lines and FBS concentrations (Table 5).

Table 5. Descriptive statistics from wound closure assays after 6 hours comparing closure between Ara-C treated and untreated cells.

		Without Ara-C				With Ara-C (1 µM)			
		N	Mean	SD	SE	N	Mean	SD	SE
SW1573									
FBS (%)	0	6	21.4	8.36	3.74	5	27.4	14.4	6.45
	1**	5	37.9	12.65	5.66	6	35.6	20.5	8.36
	2.5*	6	40.2	5.86	2.62	6	29.3	30.0	12.26
	5**	6	41.4	6.76	3.02	6	30.9	24.8	10.13
HeLa									
FBS (%)	0	6	10.8	5.77	2.58	6	10.97	5.84	2.61
	1	6	21.3	5.20	2.12	5	8.35	4.02	1.80
	2.5	6	21.5	7.08	2.89	6	12.70	6.82	3.05
	5	6	12.9	6.55	2.68	5	3.90	4.56	2.04
A549									
FBS (%)	0	6	9.50	5.85	2.93	3	11.99	3.72	2.15
	1	6	15.13	5.08	2.93	3	16.27	7.19	3.59
	2.5	6	15.43	5.46	3.15	3	9.31	6.08	3.51
	5***	6	29.40	7.56	4.37	4	8.05	6.24	3.12

*p <0.1, **p <0.05, and ***p <0.01.

In A549 cells, the treatment with Ara-C showed a significant reduction in closure (p <0.05) exclusively in the 5% FBS condition, where we have seen the highest effect of cell growth. Under the rest of conditions, no significant differences were found. For SW1573

cells, all conditions except 0% FBS were significantly different ($p < 0.1$). In addition, 1 and 5% FBS were significantly different ($p < 0.05$). These results are relevant because we observed a considerable growth effect under these conditions. In contrast, in HeLa cells no significant differences were found using Ara-C for all serum conditions even being the cell line where most cell growth effect was found in wound closure. However, for all cell lines and conditions morphological changes (Figure 5) inhibiting completely cell movement and originating cell death due to the action of Ara-C were discarded from the study. This phenomenon appeared randomly so there are probably some interactions that we are not considering. Some authors use preincubations with Ara-C, which is removed before performing the in vitro wound healing assay [27]. We cannot discard that drugs being tested interact with Ara-C or that the effect of Ara-C interferes with the action of tested drugs.

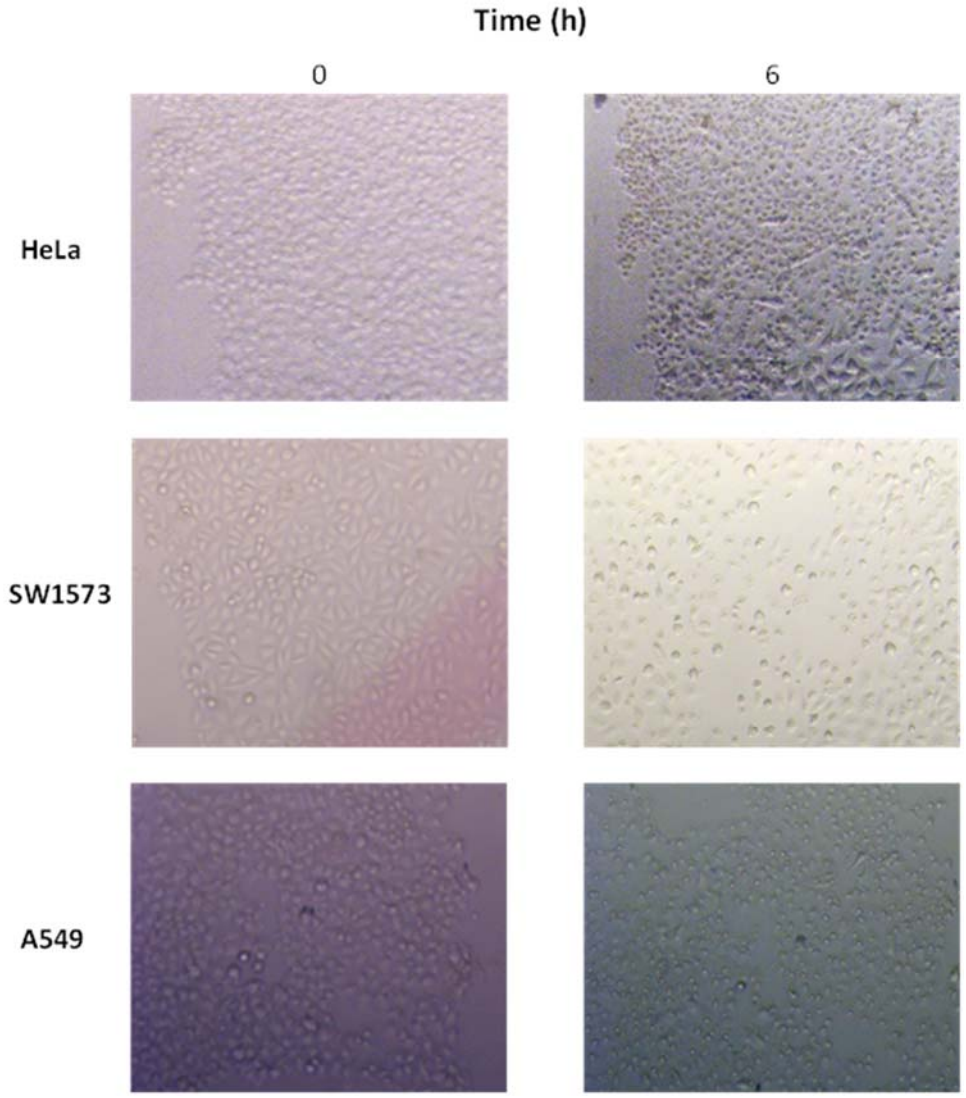

Figure 5. Representative microscopy images of the wound healing assay showing morphologic changes in cells treated with Ara-C at different time intervals.

2. Cell migration inhibition of natural extracts

Hypericum (Hypericaceae) revealed its potential as a source of new antiproliferative drugs [28]. The aerial parts of some of them have been used in traditional medicine [29]. In this study, we evaluated cell migration inhibition of methanol water (MW) fractions (which have exhibited antiproliferative activity) from extracts of four *Hypericum* species (Figure 6).

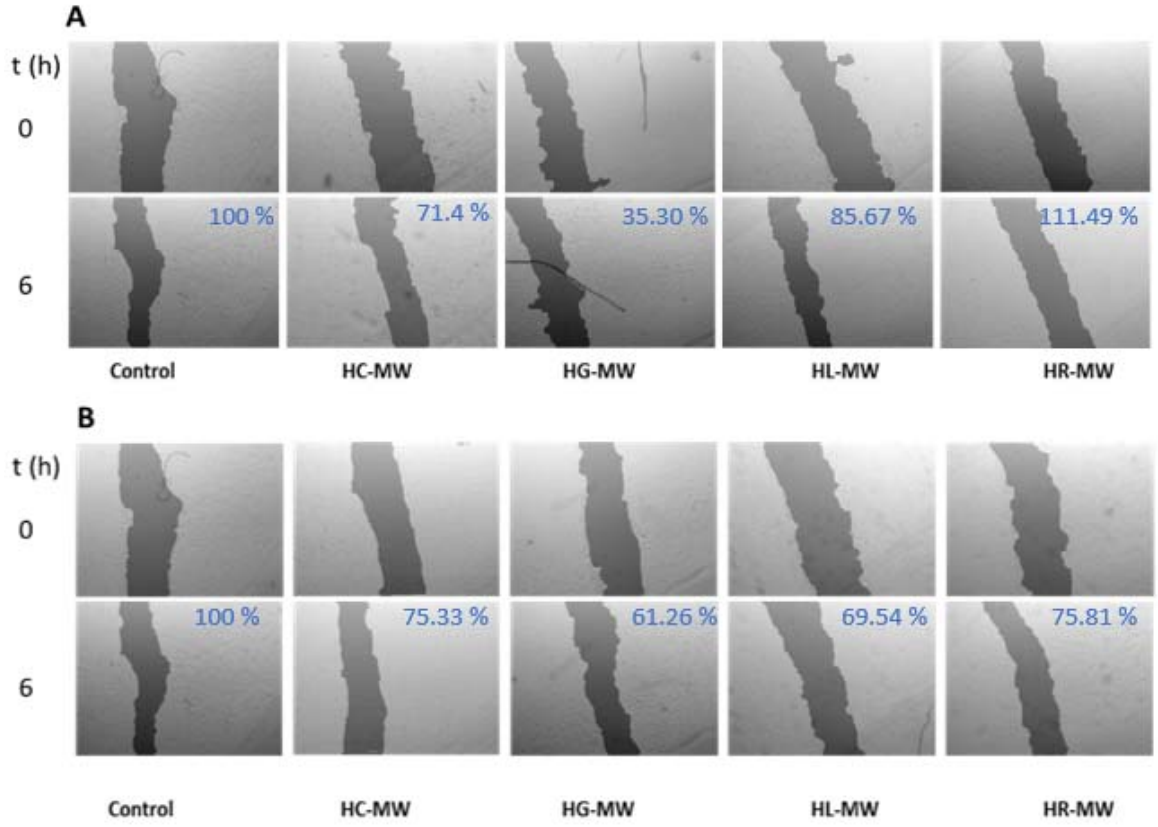

Figure 6. Wound closure assay results when using 100 µg/mL (A) and 50 µg/mL (B) of *Hypericum* extracts. Results are represented as closure percentage related to the control.

After calculating wound closure, it was standardized by comparison against the closure in the control. It was observed that the highest inhibition happened in HG-MW at 100 µg/mL where the closure was only the 35% of closure with respect to the control conditions. In contrast, for the rest of the extracts the closure was close to the control or even higher than the control. At 50 µg/mL the highest inhibition was also observed in HG-MW while the inhibition in HL-MW and HR-MW was increased. This is interesting because we can observe higher inhibition at lower dose, which is unexpected, while HC-MW seems. It is also noticeable that comparing extract with close GI_{50} concentrations in A549 cells HC-MW (GI_{50} = 89 µg/mL) does not show a relevant effect on wound closure at the assayed concentrations. Notably, HG-MW (GI_{50} = 82 µg/mL) showed the highest migration

inhibition in both concentrations. Finally, HL-MW (GI_{50} = 81 µg/mL) exhibited an increment of inhibition at lower dose. In summary, we can observe three different behaviours for extracts with similar antiproliferative activity. These differences are probably related to different mechanisms of action probably related to the different bioactive compounds present in each extract.

3. Live cell imaging

Nanolive SA CX-A live cell imaging system is a new, and label free, way to visualize phenotypic changes in cell culture. The technique represents an important advancement in drug discovery because it is possible to visualize changes happening through the time and not only at the endpoint. Phenotypic changes that happen in the cell in response to drug exposure can be observed and measured by this system and could potentially be used to identify different cell death types and mechanisms of action. In this study, we tried to develop a bioinformatic algorithm able to distinguish between mechanisms of action of different drugs. To explore this hypothesis, we selected drugs with well-stablished mechanisms of action. In particular, we focused on drugs targeting microtubules because of their natural origin. In general, there are two mechanisms of microtubule affection. Disruption of microtubule structures and hyper-stabilization of these, leading in both cases to mitotic arrest due to abnormal function of the mitotic spindle. In Figure 7, we can observe these differential phenotypic responses of three drugs with the same target but different mechanism of action. Paclitaxel is a microtubule hyper-stabilizing drug which induces mitotic arrest by binding to tubulin polymers [30]. The hyper-stabilization produced a small number of unattached kinetochores that activate the mitotic checkpoint. As shown with white arrows in Figure 7E-F, cells entering in mitosis do not assemble the mitotic spindle correctly and stay in this phase while cell that have not entered in mitosis keep a normal morphology (yellow arrows in Figure 7 E and F). Cells will either die during mitotic arrest or due to a process called slippage where cells enter directly in G_1 phase resulting in a single tetraploid cell **¡Error! No se encuentra el origen de la referencia.**. It has also been reported multipolar spindles induction as mechanism for paclitaxel. This is probably what we observed marked in circle in Figure 7F. Vinblastine and colchicine are also alkaloids, but they act destabilizing microtubules. Vinblastine is a vinca alkaloids. The vinca-binding domain on β-tubulin is located near the exchangeable GTP binding site [32]. In contrast, colchicine binds to the interphase between β and α subunits [33]. It has been reported that depolymerizing agents can induce morphologic changes in cells. For example, incubation with colchicine induces significant

decrease in the nucleus area [34]. This can be observed in Figures 7G-H and 7K marked with white arrows where we can see the nucleus collapsing and rounding probably due to the loss of the cytoskeleton. Finally, cells die from apoptosis [35] as we can see in Figure 7 I and K-L marked with white arrows.

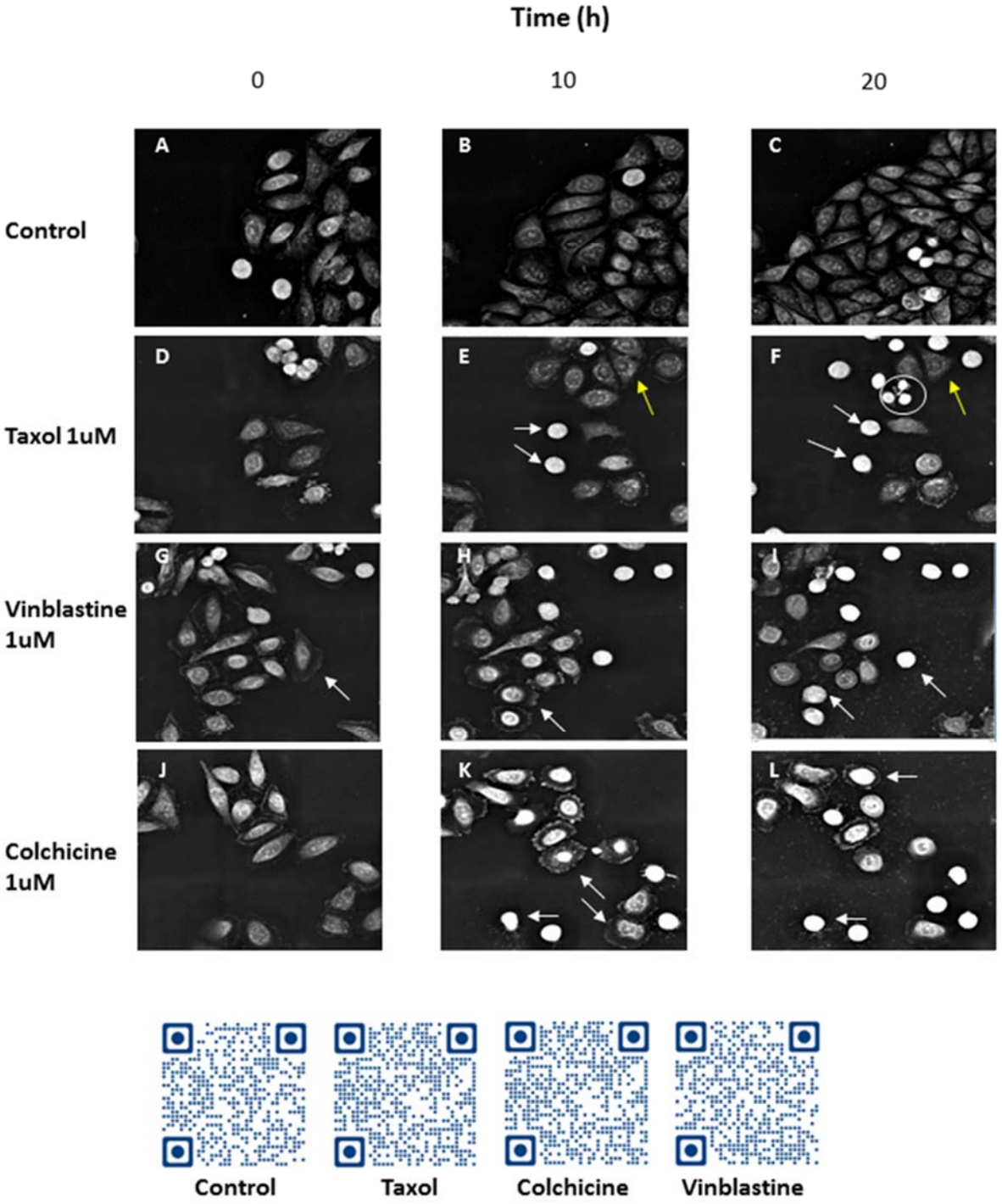

Figure 7. Images at different time intervals showing phenotypic response of SW1573 cells to drugs targeting microtubules. On the bottom QR codes for the time lapse of the different treatment.

4. Cell imaging analysis and Bioinformatic modeling.

Similarities in the phenotypic responses observed in cells when treated with compounds with different mechanisms of action were also observed in the patterns of different variables obtained from the analysis software. For example, the *Average dry mass density* (ADMD) that can be inferred from the refractive index measurements [36] has a different pattern depending on the mechanism of action of the drugs under study. Vinblastine and colchicine showed the same pattern, whilst paclitaxel displayed different features (Figure 8A). ADMD depends of dry mass (DM) and cell volume. As we can observe, DM stays quite stable for both types of compounds (Figure 8B) with a small increment in vinblastine and colchicine treatments, which shows that there is no massive leakage or accumulations of material from the cells [37]. This result suggests that changes in ADMD are happening due to changes in cell's volume.

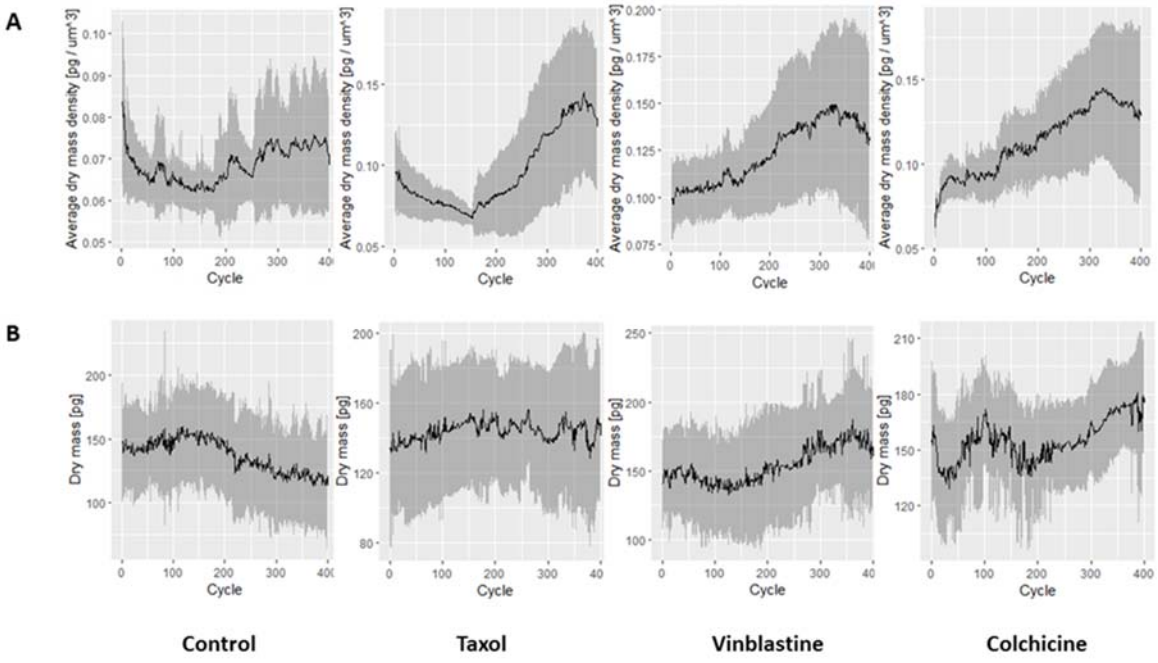

Figure 8. Time series representation of ADMD (Top row) and DM (bottom row) for different drugs tested. Gray area limit shows standard deviation. Cell number was 23 at cycle 1 and 64 at cycle 64 for the control well. Cells in paclitaxel treated n = 16. For vinblastine cell number at cycle 1 was 26 and 24 at the final cycle. For colchicine treated cells n = 16

The initial increment for paclitaxel turns into a steep increment from the cycle 200 onwards. This could be related to the entrance of the cells in mitosis were a considerable cell condensation happens reducing cell volume and the ADMD. In cells treated with microtubule

disruptors, the increment in ADMD starts from the beginning and progresses through exposure (Figure 8A). This could be explained by the shrinkage that happens to the cell due to the cytoskeleton disruption. Something similar happens with cell area changes (Figure 9). The use of paclitaxel induces a drastic cell area decrement from the cycle 200 onwards probably due to cells entering in mitotic arrest while vinblastine and colchicine induced smooth area reduction.

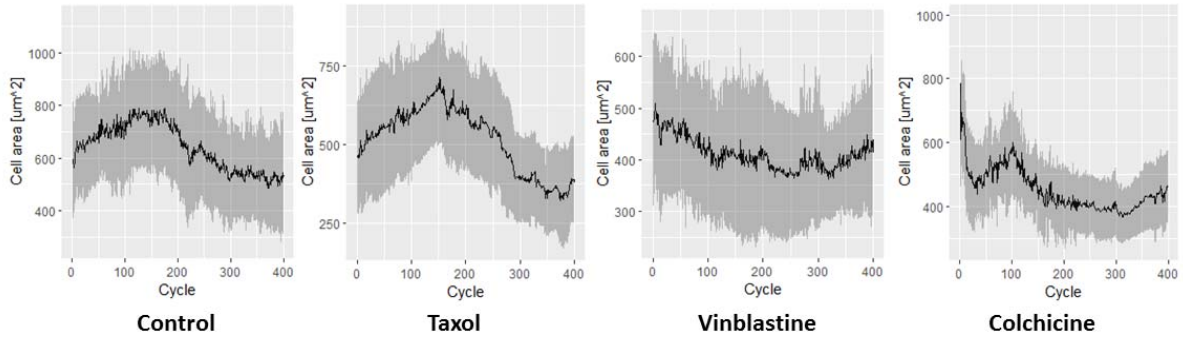

Figure 9. Time series representation of Cell area for different drugs tested. Gray area limit shows standard deviation.

Commonly, the time series are visually similar to waveform functions at different points. The Fourier transform (FT) is a mathematical function that decomposes a waveform, which is a function of time into the frequencies that make it up. At the end, FT allows viewing a function as a sum of simple sinusoids (Figure 10) with different amplitudes and corresponding phases. Notice that the amplitudes and corresponding phases are unique for each function. Thus, we can observe differences between ADMD and DM in amplitude composition. In both cases, the highest amplitudes are found in the first and final cycles. Attending to the phase corresponding to those amplitudes, we can observe that in the beginning the highest amplitudes correspond to a positive phase in ADMD and a negative phase corresponds to the highest amplitude in the final cycles. In those at the final cycles, the correspondence is with negative phases. This may be a reflect of the behavior of these measurements in the time series (Figure 8), where we could observe that ADMD decreases at the initial cycles and then increases. In contrast, DM behaved opposite having first a slight increase and then decreasing until the final cycle. In the case of these measurements (DM and ADMD), Table 6 shows how maximal amplitude changes depending on the treatment. There are also changes in the corresponding phase. Thus, it can be used as a variable to compare the different conditions.

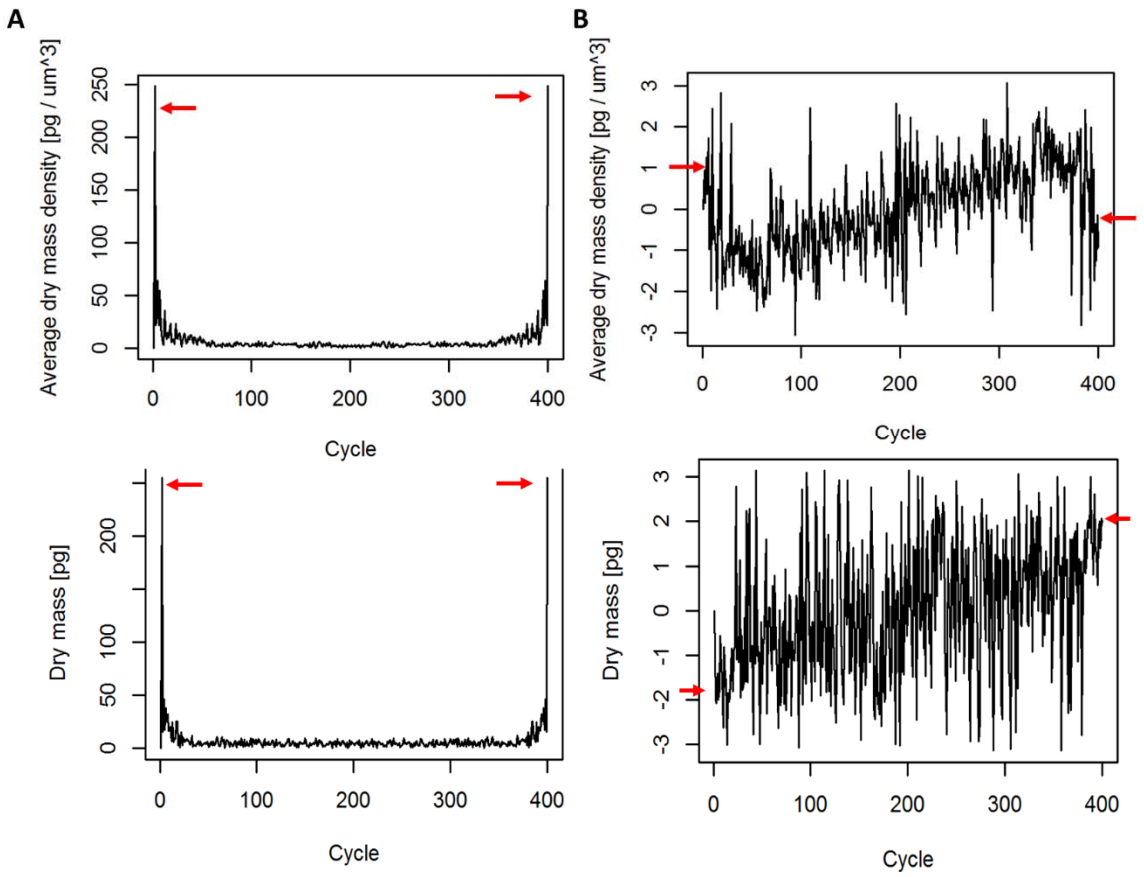

Figure 10. (A) Representation of the amplitudes from the sinusoids composing Dry mass and Dry mass density in control conditions. (B) Phases corresponding to the different amplitudes. Red arrows mark highest amplitudes and corresponding phases.

Table 6. Representation of maximum amplitude and corresponding phase of ADMD and DM after applying FT.

		Maximum amplitude	Phase
Control			
	Average dry mass density	248.98	0.94
	Dry mass	255.06	-1.98
Paclitaxel			
	Average dry mass density	260.13	0.99
	Dry mass	155.40	3.05
Viblastine			
	Average dry mass density	255.65	1.64
	Dry mass	250.17	1.17
Colchicine			
	Average dry mass density	240.96	1.66
	Dry mass	152.82	2.09

Once selected the maximum amplitudes (Figure 11) and the corresponding phases, we could observe that in many variables the highest amplitude of the similar compounds are also the most similar and their phases are also the most similar.

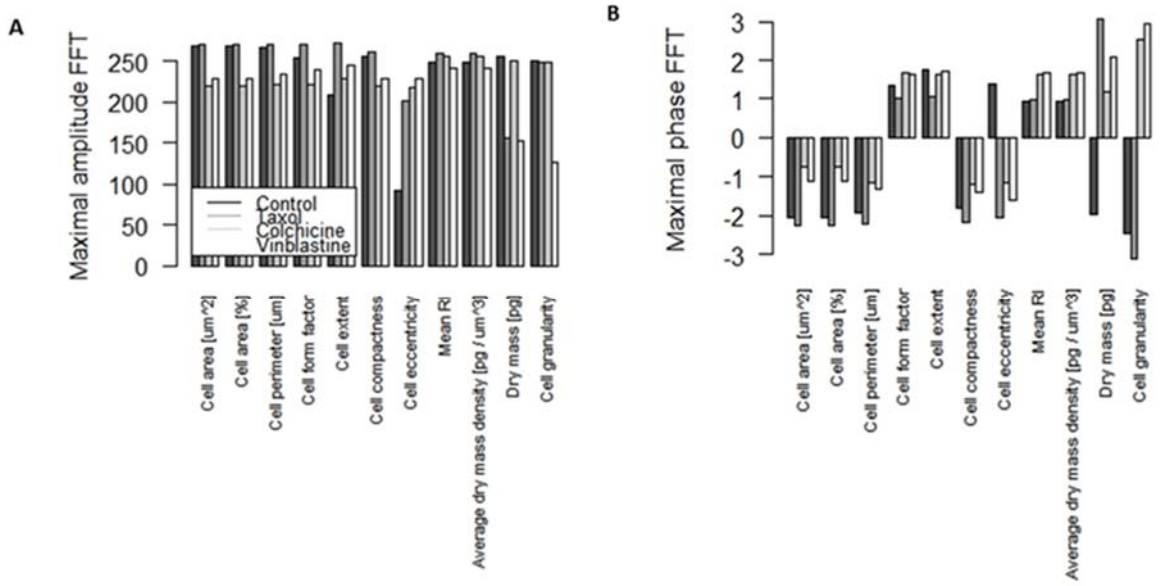

Figure 11. (A) Graphical representation of maximum amplitudes for the different measurements and conditions. (B) Corresponding phase to maximal amplitude

The heat map (Figure 12) clustered compounds with the same mechanism of action (microtubule disruption) which are colchicine and vinblastine. Even though this clustering had 25% possibilities because of the use of 4 conditions. The groups formed are a good preliminary result for our prediction model. More compounds with this and different mechanism of action need to be tested. Also, testing compounds in other cell lines would give more information and strength to the algorithm. The calculation of FT for each cell instead of mean values can help giving the possibility of screening outliers and asses biological variability and differential response to tested drugs.

Further development requires the identification of the variables that are more important in the clustering of the treatments. Probably, using a principal components analysis, a technique for reducing the dimensionality of such datasets, increasing interpretability but at the same time minimizing information loss might enhance the algorithm [38]. Finally, it would potentially be possible to establish a mathematical model for predicting the mechanism of action.

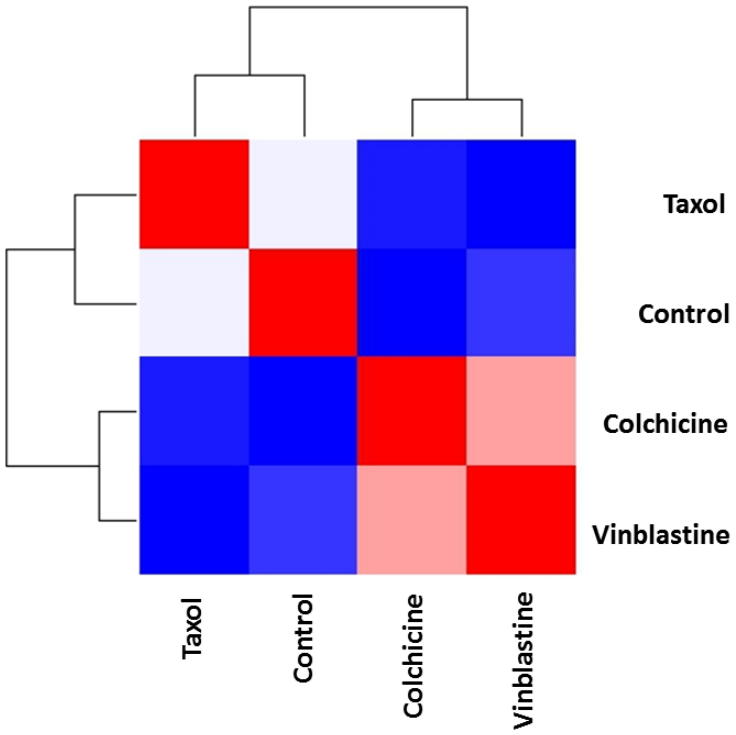

Figure 12. Heat map representing the correlation and clustering between the different compounds. Positive correlation is marked in red while negative correlation is shown in blue. The treatments with highest positive correlation (most similar) appear clustered.

Considering the limitations of these study, the obtained results represent a good preliminary outcome that makes us confident about the proposed model. In essence, our model might aid to integrate label free cell imaging and analysis system into phenotypic drug discovery programs.

CONCLUSIONS

1. Cell migration studies can be evaluated after 6 hours of wound formation.
2. A549 cells at 1% FBS represent the optimum model to evaluate cell migration.
3. HG-MW extract inhibits drastically cell migration.
4. Live cell imaging can distinguish differential phenotypic changes related to drugs.
5. Our first version of the algorithm seem to differentiate microtubule disruptors from hyperstabilizing drugs.

CONCLUSIONES

1. Observamos que la migración celular se puede estudiar a 6h.
2. Observamos que A549 con 1% FBS es el modelo más óptimo para evaluar la migración celular.
3. El extracto de HG-MW inhibe drásticamente la migración celular.
4. El sistema de imagen celular en vivo permite distinguir cambios fenotípicos relacionados con fármacos.
5. El algoritmo diseñado es capaz de diferenciar fármacos disruptores de microtúbulos de fármacos hiper-estabilizantes.

REFERENCES

[1] Buckner, C. A., Lafrenie, R. M., Dénommée, J. A., Caswell, J. M., Want, D. A., Gan, G. G., Leong, Y. C., Bee, P. C., Chin, E., Teh, A. K. H., Picco, S., Villegas, L., Tonelli, F., Merlo, M., Rigau, J., Diaz, D., Masuelli, M., Korrapati, S., Kurra, P., Mathijssen, R. H. J. (2016). *Intech*, *11*(tourism), 13.

[2] Newman, D. J., & Cragg, G. M. (2020). Natural Products as Sources of New Drugs over the Nearly Four Decades from 01/1981 to 09/2019. *Journal of Natural Products*, *83*(3), 770–803. https://doi.org/10.1021/acs.jnatprod.9b01285

[3] Krishnan, R., Singh, S. P., & Upadhyay, S. K. (2021). An Introduction to Plant Biodiversity and Bioprospecting. *Bioprospecting of Plant Biodiversity for Industrial Molecules*, 1–13. https://doi.org/10.1002/9781119718017.ch1

[4] Huang, M., Lu, J. J., & Ding, J. (2021). Natural Products in Cancer Therapy: Past, Present and Future. *Natural Products and Bioprospecting*, *11*(1), 5–13. https://doi.org/10.1007/s13659-020-00293-7

[5] Huang, M., Lu, J. J., & Ding, J. (2021). Natural Products in Cancer Therapy: Past, Present and Future. *Natural Products and Bioprospecting*, *11*(1), 5–13. https://doi.org/10.1007/s13659-020-00293-7

[6] Moffat, J. G., Rudolph, J., & Bailey, D. (2014). Phenotypic screening in cancer drug discovery-past, present and future. *Nature Reviews Drug Discovery*, *13*(8), 588–602. https://doi.org/10.1038/nrd4366

[7] Moffat, J. G., Rudolph, J., & Bailey, D. (2014). Phenotypic screening in cancer drug discovery-past, present and future. *Nature Reviews Drug Discovery*, *13*(8), 588–602. https://doi.org/10.1038/nrd4366

[8] Hanahan, D., & Weinberg, R. A. (2011). Hallmarks of cancer: The next generation. *Cell*, *144*(5), 646–674. https://doi.org/10.1016/j.cell.2011.02.013

[9] Whitby, L. R., Obach, R. S., Simon, G. M., Hayward, M. M., & Cravatt, B. F. (2017). Quantitative Chemical Proteomic Profiling of the in Vivo Targets of Reactive Drug Metabolites. *ACS Chemical Biology*, *12*(8), 2040–2050. https://doi.org/10.1021/acschembio.7b00346

[10] Friedl, P., & Wolf, K. (2003). Tumour-cell invasion and migration: Diversity and escape mechanisms. *Nature Reviews Cancer*, *3*(5), 362–374. https://doi.org/10.1038/nrc1075

[11] Roche, J. (2018). The epithelial-to-mesenchymal transition in cancer. *Cancers*, *10*(2), 10–13. https://doi.org/10.3390/cancers10020052

[12] Wang, X., Decker, C. C., Zechner, L., Krstin, S., & Wink, M. (2019). In vitro wound healing of tumor cells: Inhibition of cell migration by selected cytotoxic alkaloids. *BMC Pharmacology and Toxicology*, *20*(1), 1–12. https://doi.org/10.1186/s40360-018-0284-4

[13] Moreno, H., Archetti, L., Gibbin, E., Grandchamp, A. E., & Fréchin, M. (2021). Artificial Intelligence-Powered Automated Holotomographic Microscopy Enables Label-Free Quantitative Biology. *Microscopy Today*, *29*(5), 24–32. https://doi.org/10.1017/s1551929521001139

[14] Boyd, M. R. (2004). The NCI Human Tumor Cell Line (60-Cell) Screen. *Anticancer Drug Development Guide*, 41–61. https://doi.org/10.1007/978-1-59259-739-0_3

[15] Bates, S. E., Fojo, A. T., Weinstein, J. N., Myers, T. G., Alvarez, M., Pauli, K. D., & Chabner, B. A. (1995). Molecular targets in the National Cancer Institute drug screen. *Journal of Cancer Research and Clinical Oncology*, *121*(9–10), 495–500. https://doi.org/10.1007/BF01197759

[16] Jonkman, J. E. N., Cathcart, J. A., Xu, F., Bartolini, M. E., Amon, J. E., Stevens, K. M., & Colarusso, P. (2014). An introduction to the wound healing assay using live-cell microscopy. In *Cell Adhesion and Migration* (Vol. 8, Issue 5, pp. 440–451). Landes Bioscience. https://doi.org/10.4161/cam.36224

[17] Gebäck, T., Schulz, M. M. P., Koumoutsakos, P., & Detmar, M. (2009). TScratch: A novel and simple software tool for automated analysis of monolayer wound healing assays. *BioTechniques*, *46*(4), 265–274. https://doi.org/10.2144/000113083

[18] The jamovi project (2021). *jamovi*. (Version 1.6) [Computer Software]. Retrieved from https://www.jamovi.org.

[19] RStudio Team (2022). *RStudio*: Integrated Development Environment for R. RStudio, PBC, Boston, MA URL http://www.rstudio.com/.

[20] Wang, S. (2017). Applications of Fourier Transform to Imaging Analysis. *Journal of the Royal Statistical Society*, *5*, 1–11. http://pages.stat.wisc.edu/~mchung/teaching/MIA/projects/FT_complex.pdf

[21] Bobadilla, A. V. P., Arévalo, J., Sarró, E., Byrne, H. M., Maini, P. K., Carraro, T., Balocco, S., Meseguer, A., & Alarcón, T. (2019). In vitro cell migration quantification method for scratch assays. *Journal of the Royal Society Interface*, *16*(151). https://doi.org/10.1098/rsif.2018.0709

[22] Liang, C.-C., Park, A. Y., & Guan, J.-L. (2007). In vitro scratch assay: a convenient and inexpensive method for analysis of cell migration in vitro. *Nature Protocols*, *2*(2), 329–333. https://doi.org/10.1038/nprot.2007.30

[23] Herbst, R. S., Morgensztern, D., & Boshoff, C. (2018). The biology and management of non-small cell lung cancer. *Nature*, *553*(7689), 446–454. https://doi.org/10.1038/nature25183

[24] Shintani, Y., Okimura, A., Sato, K., Nakagiri, T., Kadota, Y., Inoue, M., Sawabata, N., Minami, M., Ikeda, N., Kawahara, K., Matsumoto, T., Matsuura, N., Ohta, M., & Okumura, M. (2011). Epithelial to mesenchymal transition is a determinant of sensitivity to chemoradiotherapy in non-small cell lung cancer. *Annals of Thoracic Surgery*, *92*(5), 1794–1804. https://doi.org/10.1016/j.athoracsur.2011.07.032

[25] Puri, N., Pitman, R. T., Mulnix, R. E., Erickson, T., Iness, A. N., Vitali, C., Zhao, Y., Salgia, R. (2018). *HHS Public Access*. *343*(1), 14–23. https://doi.org/10.1016/j.canlet.2013.09.010.Non-small

[26] Sun, F., Li, N., Tong, X., Zeng, J., He, S., Gai, T., Bai, Y., Liu, L., Lu, K., Shen, J., Han, M., Lu, C., & Dai, F. (2019). Ara-c induces cell cycle G1/S arrest by inducing upregulation of the INK4 family gene or directly inhibiting the formation of the cell cycle-dependent complex CDK4/cyclin D1. *Cell Cycle*, *18*(18), 2293–2306. https://doi.org/10.1080/15384101.2019.1644913

[27] Giretti, M. S., Guevara, M. M. M., Cecchi, E., Mannella, P., Palla, G., Spina, S., Bernacchi, G., Di Bello, S., Genazzani, A. R., Genazzani, A. D., & Simoncini, T. (2014). Effects of estetrol on migration and invasion in T47-D breast cancer cells through the actin cytoskeleton. *Frontiers in Endocrinology*, *5*(MAY), 1–8. https://doi.org/10.3389/fendo.2014.00080

[28] Bridi, H., Meirelles, G. de C., & von Poser, G. L. (2018). Structural diversity and biological activities of phloroglucinol derivatives from Hypericum species. *Phytochemistry*, *155*(October 2017), 203–232. https://doi.org/10.1016/j.phytochem.2018.08.002

[29] DE PAZ, Pedro L. Pérez; PADRÓN, Consuelo E. Hernández. *Plantas medicinales o útiles en la flora canaria: aplicaciones populares*. F. Lemus, 1999.

[30] Parness, J., & Horwitz, S. B. (1981). Paclitaxel binds to polymerized tubulin in vitro. *Journal of Cell Biology*, *91*(2 I), 479–487. DOI: 10.1083/jcb.91.2.479

[31] Zasadil, L. M., Andersen, K. A., Yeum, D., Rocque, G. B., Wilke, L. G., Tevaarwerk, A. J., Raines, R. T., Burkard, M. E., & Weaver, B. A. (2014). Cytotoxicity of paclitaxel in breast cancer is due to chromosome missegregation on multipolar spindles. *Science Translational Medicine*, *6*(229). DOI: 10.1126/scitranslmed.3007965

[32] Perez, E. A. (2009). Microtubule inhibitors: Differentiating tubulin-inhibiting agents based on mechanisms of action, clinical activity, and resistance. *Molecular Cancer Therapeutics*, *8*(8), 2086–2095. https://doi.org/10.1158/1535-7163.MCT-09-0366

[33] Banerjee, S., Hwang, D. J., Li, W., & Miller, D. D. (2016). Current advances of tubulin inhibitors in nanoparticle drug delivery and vascular disruption/angiogenesis. *Molecules*, *21*(11). https://doi.org/10.3390/molecules21111468

[34] Weber, A., Iturri, J., Benitez, R., Zemljic-Jokhadar, S., & Toca-Herrera, J. L. (2019). Microtubule disruption changes endothelial cell mechanics and adhesion. *Scientific Reports*, *9*(1), 1–12. https://doi.org/10.1038/s41598-019-51024-z

[35] Yang, M., Jiang, P., & Hoffman, R. M. (2015). Early reporting of apoptosis by real-time imaging of cancer cells labeled with green fluorescent protein in the nucleus and red fluorescent protein in the cytoplasm. *Anticancer Research*, *35*(5), 2539–2544.

[36] Aknoun, S., Savatier, J., Bon, P., Galland, F., Abdeladim, L., Wattellier, B., & Monneret, S. (2015). Living cell dry mass measurement using quantitative phase imaging with quadriwave lateral shearing interferometry: an accuracy and sensitivity discussion. *Journal of Biomedical Optics*, *20*(12), 126009. https://doi.org/10.1117/1.jbo.20.12.126009

[37] Moreno, H., Archetti, L., Gibbin, E., Grandchamp, A. E., & Fréchin, M. (2021). Artificial Intelligence-Powered Automated Holotomographic Microscopy Enables Label-Free Quantitative Biology. *Microscopy Today*, *29*(5), 24–32. https://doi.org/10.1017/s1551929521001139

[38] Jollife, I. T., & Cadima, J. (2016). Principal component analysis: A review and recent developments. *Philosophical Transactions of the Royal Society A: Mathematical, Physical and Engineering Sciences*, *374*(2065). https://doi.org/10.1098/rsta.2015.0202